CSIRO PUBLISHING

Aust. J. Chem. **2012**, *65*, 160–168
http://dx.doi.org/10.1071/CH11420

Full Paper

Dual-Level Direct Dynamics Studies on the Hydrogen Abstraction Reactions of $CH_2CH_{3-n}X_n + HBr$ (X = Cl, Br and $n = 1, 2$)

Li Wang,[A] *Jianxiang Zhao,*[A] *Hongqing He,*[B] *and Jinglai Zhang*[A,C]

[A]Institute of Environmental and Analytical Sciences, College of Chemistry and Chemical Engineering, Henan University, Kaifeng, Henan 475004, P. R. China.
[B]Wuhan Center for Magnetic Resonance, State Key Laboratory of Magnetic Resonance and Atomic and Molecular Physics, Wuhan Institute of Physics and Mathematics, Chinese Academy of Sciences, Wuhan 430071, P. R. China.
[C]Corresponding author. Email: zhangjinglai@henu.edu.cn

The reactions of the HBr molecule with CH_2CH_2Cl (reaction R1), CH_2CHCl_2 (R2), CH_2CH_2Br (R3) and CH_2CHBr_2 (R4) are investigated by a dual-level direct dynamics method. The optimized geometries and frequencies of the stationary points were calculated at the MPW1K/6–311+G(d,p) and BMK/6–311+G(d,p) levels. To refine the reaction enthalpy and energy barrier height of each reaction, single-point energy calculations were carried out by the G2M(RCC5) method based on the geometries optimized at the above-mentioned two levels. Using the canonical variational transition state theory or the canonical variational transition state theory with the small-curvature tunneling correction, the rate constants of HBr with CH_2CH_2Cl (R1), CH_2CHCl_2 (R2), CH_2CH_2Br (R3), and CH_2CHBr_2 (R4) were calculated over a wide temperature range of 200–2000 K at the G2M(RCC5)//MPW1K/6–311+G(d,p) level. The effect of chlorine or bromine substitution on the ethyl radical reactivity is discussed. Finally, the total rate constants are fitted by two models, i.e. three-parameter and four-parameter expressions.

Manuscript received: 27 October 2011.
Manuscript accepted: 21 December 2011.
Published online: 1 February 2012.

Introduction

Chlorine, as part of an organic compound, plays an important and essential role in combustion processes of chlorine-bearing polymeric materials. The chlorine atom has very high reactivity and a tendency to react with saturated hydrocarbons by a hydrogen-atom abstraction reaction and with unsaturated hydrocarbons by a pressure-dependent addition reaction.[1,2] The abstraction reaction with unsaturated hydrocarbons produces free radicals at low temperatures. Then, they will react with other atmospheric atoms and molecules. During the past three decades, extensive studies of the photochlorination of ethylene and its derivatives have contributed much to our understanding of the reactions of chloroethyl radicals.[3–6] In contrast, few investigations of the analogous bromination and hydrobromination reactions have been reported, especially for bromoethyl radicals.

There is only one previous report on the temperature dependence of the rate constant of the reaction $HBr + CH_2CH_2Cl$ (reaction R1) from 300 to 409 K. Seetula's results were fitted to a linear Arrhenius plot with a pre-exponential factor $A = (5.7 \pm 1.6) \times 10^{-13}$ cm^3 molecule^{-1} s^{-1} and a slight negative activation energy $E_a = -2.22 \pm 0.79$ kJ mol^{-1}.[7] As for the reaction $CH_2CH_2Br + HBr \rightarrow CH_3CH_2Br + Br$ (R3), only the relative rate constants were reported.[8] Until now, no absolute rate constants have been reported. To the best of our knowledge, no experimental or theoretical investigation has been performed on two other reactions: $CH_2CHCl_2 + HBr \rightarrow CH_3CHCl_2 + Br$ (R2) and $CH_2CHBr_2 + HBr \rightarrow CH_3CHBr_2 + Br$ (R4). The general purpose of this paper is to gain an insight into the dynamic properties of reactions of HBr with four chlorinated or brominated ethyl radicals and provide a reliable prediction of the rate constants over a wide temperature range. Specifically, we will focus on the reactivity trend of four reactions. Our results may be particularly useful for reactions R2–R4 for which no experimental rate constant has been measured.

The dynamic properties were studied by a dual-level approach (X//Y).[9–13] Part of the potential energy surface was obtained from the electronic structure calculation, and the rate constants were calculated by means of the *POLYRATE 9.7* program[14] using the variational transition-state theory (VTST).[15–17]

Results and Discussion

Stationary Points

The geometric parameters of the reactants, products, complexes and transition states optimized at the MPW1K/6–311+G(d,p) and BMK/6–311+G(d,p) levels as well as the available experimental values are listed in Fig. 1. The Cartesian coordinates and electronic energies for MPW1K/6–311+G(d,p)- and BMK/6–311+G(d,p)-optimized geometries of all stationary points are listed in Tables S1 and S2 in the Supplementary Material

respectively. The optimized parameters obtained at the two levels were observed to agree. The largest discrepancy was 0.1 Å for the calculated bond lengths and 2° for the angles. Moreover, the theoretical values are in reasonable agreement with the experimental values[18–20] to within a maximum error of 2.7 %. In addition, owing to the electronegativity of the carbon atom, chlorine atom and bromine atom, hydrogen-bonded complexes are found at the beginning or end of reactions. At the

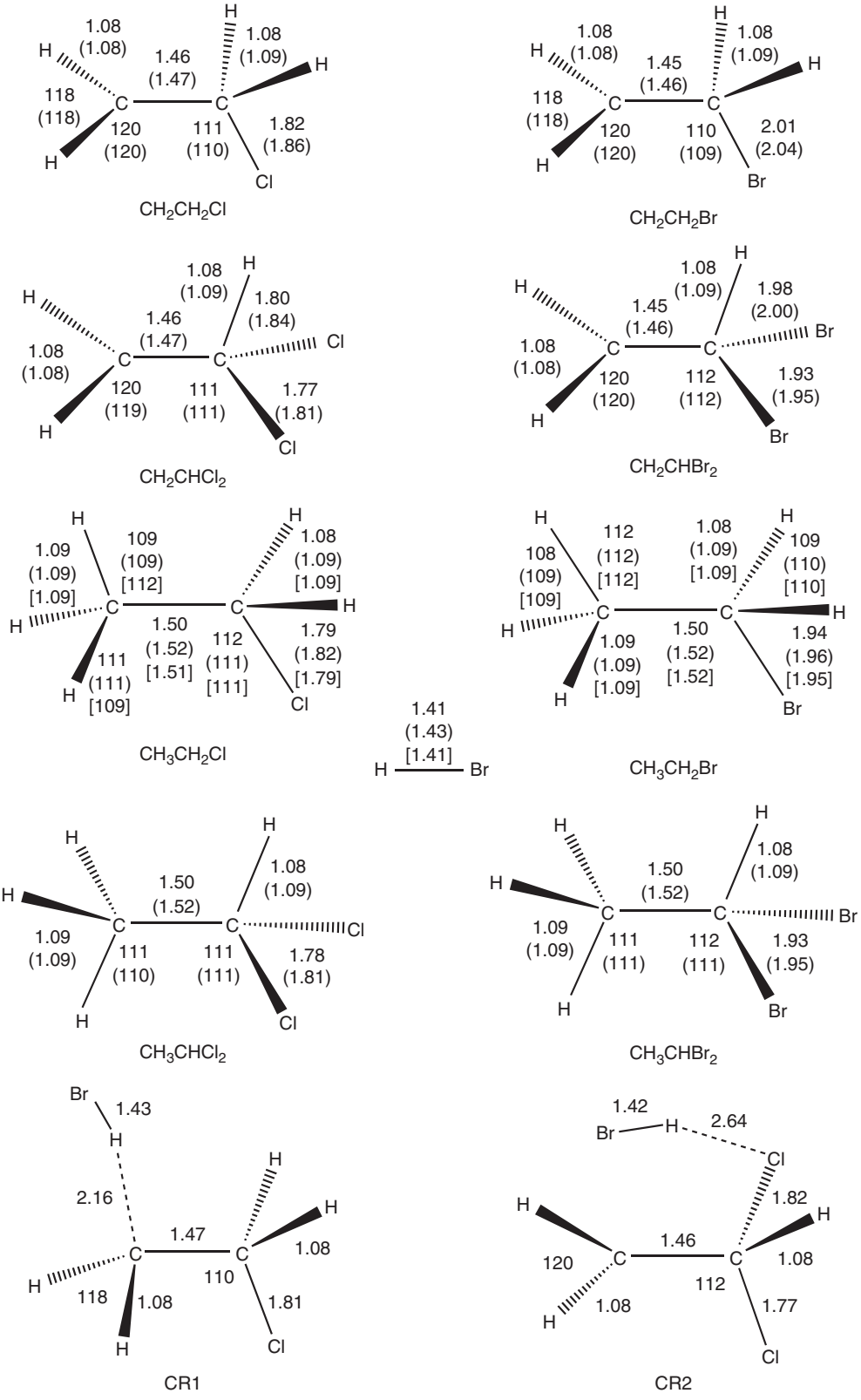

Fig. 1. Optimized geometries of reactants, products, complexes and transition states at the MPW1K/6–311+G(d,p) level. The values in parentheses and square brackets are the values calculated at the BMK/6–311+G(d,p) level and experimental values[18–20] respectively. Bond lengths are in angstroms and angles are in degrees.

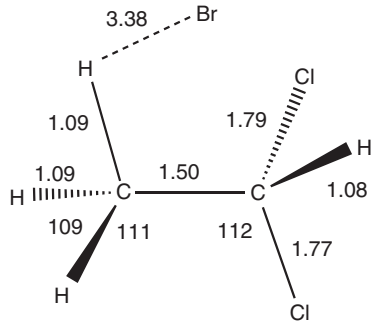

CP2

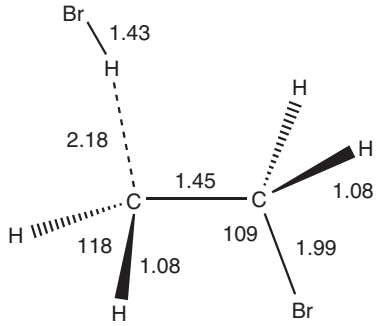

CR3

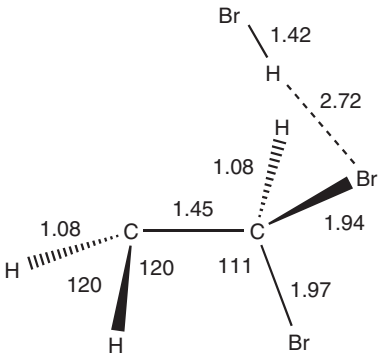

CR4

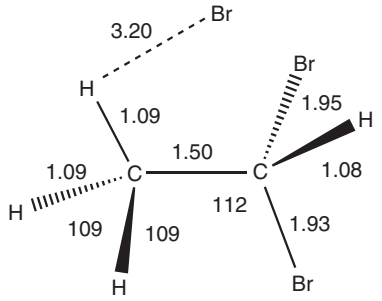

CP4

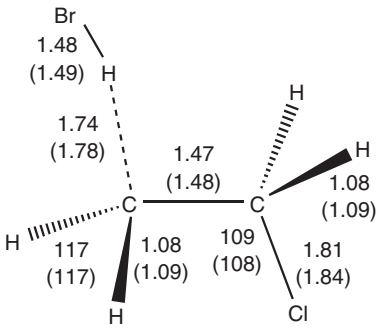

TS1

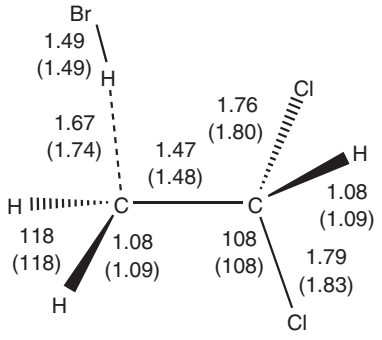

TS2

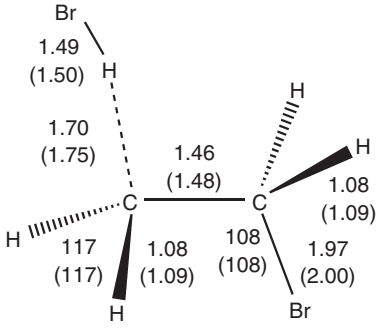

TS3

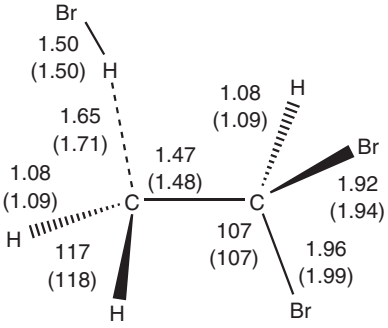

TS4

Fig. 1. (*Continued*)

MPW1K/6–311+G(d,p) level, the elongation of breaking H–Br bonds are 5.0, 5.7, 5.7 and 6.4 % respectively; and the forming C–H bonds are stretched by 59.6, 53.2, 56.0 and 51.4 % compared with the equilibrium bond length in isolated CH_3CH_2Cl, CH_3CHCl_2, CH_3CH_2Br, and CH_3CHBr_2 respectively. The elongation of the forming bond is much greater than that of the breaking bond, indicating that the transition states are reactant-like, i.e. all these reactions proceed via 'early' transition states,

Table 1. Reaction enthalpies (in kJ mol^{-1}) at the MPW1K/6–311+G(d,p), BMK/6–311+G(d,p), G2M(RCC5)//MPW1K/6–311+G(d,p) and G2M(RCC5)//BMK/6–311+G(d,p) levels with the experimental values

	$CH_2CH_2Cl + HBr \rightarrow CH_3CH_2Cl + Br$	$CH_2CHCl_2 + HBr \rightarrow CH_3CHCl_2 + Br$	$CH_2CH_2Br + HBr \rightarrow CH_3CH_2Br + Br$	$CH_2CHBr_2 + HBr \rightarrow CH_3CHBr_2 + Br$
MPW1K/6–311+G(d,p)	−43.76	−48.99	−37.24	−42.13
G2M(RCC5)//MPW1K/6–311+G(d,p)	−51.08	−57.18	−44.22	−50.16
BMK/6–311+G(d,p)	−57.14	−63.11	−50.49	−56.01
G2M(RCC5)//BMK/6–311+G(d,p)	−51.16	−57.60	−44.35	−50.12
Experimental[A]	−53.12 ± 16.34	−69.87 ± 1.89	−47.77 ± 8.36	

[A]From refs [20, 23, 24].

as expected for exothermic reactions. Similar character can be concluded from the geometrical structures optimized at the BMK/6–311+G(d,p) level.

The harmonic vibrational frequencies of all the stationary points along with the available experimental data[20,21] are listed in Table S3 in the Supplementary Material. Note that the MPW1K/6–311+G(d,p) and BMK/6–311+G(d,p) directly calculated frequencies were scaled by the factors of 0.969 and 0.984 reported by Alecu et al.[22] The frequencies calculated at both levels show good consistency with the available experimental values, with the largest deviation being ~10 %. All of the minima including reactants, products and complexes correspond to real frequencies, but the transition states (TSs) were confirmed to have only one imaginary (*i*) frequency, which took the values of 113*i* (TS1), 194*i* (TS2), 127*i* (TS3), and 207*i* (TS4) at the MPW1K level and the corresponding values were 167*i*, 177*i*, 135*i* and 174*i* at the BMK level.

The reaction enthalpies at 298 K (ΔH^0_{298}) (in kJ mol^{-1}) calculated at the MPW1K/6–311+G(d,p), BMK/6–311+G(d,p), G2M(RCC5)//MPW1K/6–311+G(d,p) and G2M(RCC5)//BMK/6–311+G(d,p) levels are summarised in Table 1 along with the available experimental results. As shown in Table 1, the calculated reaction enthalpies were −51.08, −57.18, −44.22 and −50.16 kJ mol^{-1}at the G2M(RCC5)//MPW1K/6–311+G(d,p) level for reactions R1–R4 respectively, and they were −51.16, −57.60, −44.35 and −50.12 kJ mol^{-1} at the G2M(RCC5)//BMK/6–311+G(d,p) level. The reaction enthalpies calculated at the two higher levels agree well for all reactions. Moreover, the ΔH^0_{298} values of reactions R1 and R3 are in good agreement with the experimental values of −53.13 ± 16.34 and −47.78 ± 8.36 kJ mol^{-1} respectively, whereas the ΔH^0_{298} values of reaction R2 calculated at both higher levels are slightly lower than the experimental value of −69.89 ± 1.88 kJ mol^{-1}. The experimental values were derived from the experimental standard heats of formation[20,23,24] (HBr, −36.24 kJ mol^{-1}; Br, 111.61 kJ mol^{-1}; CH_2CH_2Cl, 91.96 ± 8.36 kJ mol^{-1}; CH_3CH_2Cl, −109.01 ± 7.98 kJ mol^{-1}; CH_2CHCl_2, 90.1 ± 0.8 kJ mol^{-1}; CH_3CHCl_2, −127.62 ± 1.09 kJ mol^{-1}; CH_2CH_2Br, 133.76 ± 8.36 kJ mol^{-1}; CH_3CH_2Br, −61.86 kJ mol^{-1}). Comparison between theory and experiment for the enthalpy of reaction R4 is difficult because of the absence of experimentally determined enthalpy of formation values for the CH_2CHBr_2 and CH_3CHBr_2 species. However, in view of the good agreement obtained above for other three reactions, it is expected that the calculated enthalpy of reaction R4 is reliable.

A schematic potential energy surface of the title reactions with ZPE corrections is plotted in Fig. 2. Note that the energy of reactant R is set to zero as a reference. For all reactions, the hydrogen-bonded complexes CR1–CR4 with relative energies −4.72, −10.37, −5.10, and −7.94 kJ mol^{-1} at the G2M(RCC5)//MPW1K/6–311+G(d,p) level are first formed, followed by a reactant-like transition state to form the products or another complex located at the end. In complexes CR1 and CR2, hydrogen bonds are formed between an H atom of HBr and a C atom of CH_2CH_2Cl and between an H atom of HBr and a Cl atom of CH_2CHCl_2 respectively. As the electronegativity of the Cl atom is stronger than that of the C atom, complex CR2 is more stable than complex CR1. Similarly, hydrogen bonds are formed between the H atom of HBr and a C atom of CH_2CH_2Br and between the H atom of HBr and a Br atom of CH_2CHBr_2 in complexes CR3 and CR4 respectively. So complex CR4 is more stable than complex CR3.

It is obvious from Fig. 2 that the barrier height of R1 is lower than that of R2 (−1.55 versus 1.17 kJ mol^{-1}), i.e. the barrier height increases with increasing chlorine substitution. Similarly, the barrier height of R4 (2.17 kJ mol^{-1}) is higher than that of R3 (−0.71 kJ mol^{-1}). A possible reason for the decreasing reactivity with increasing halogen substitution may be the difference in atom electronegativities between halogen (Cl or Br) and H atoms. The halogen atom (Cl or Br) is more electronegative than the H atom and thus has a stronger tendency to draw electrons from the carbon atom. This phenomenon is strongest at the α position and weaker at the β position because of the distance from the radical centre. Thus, it is obvious that the electron-withdrawing tendency of the halogen atom(s) from the radical centre becomes weaker in the following order: β, β-$C_2H_3X_2$ > β-C_2H_4X > C_2H_5 (X = Cl or Br). The reverse trend is found for their reactivities. Thus, the reactivity of CH_3CH_2 radicals decreases with increasing halogen substitution.

As the determination of the transition-state structure of a reaction is essential to understanding the reaction mechanism involved, the geometries of all reactions were optimized at two levels, i.e. MPW1K and BMK, with the 6–311+G(d,p) basis set. Owing to the system including chlorine and bromine atoms, the geometries of the above-mentioned four reactions were also optimized at the MPW1K level with the 6–311+G(2df,2p) and ma-TZVP[25] basis sets respectively. The Cartesian coordinates and electronic energies for MPW1K/6–311+G(2df,2p) and MPW1K/ma-TZVP optimized geometries of all stationary points are listed in Tables S4 and S5 in the Supplementary Material respectively. Then, the barrier heights were refined by the G2M(RCC5) method. The corresponding results are listed in Table 2. As can be seen from Table 2, the barrier heights refined by the same composite method on the different geometries are consistent, with a maximum error within 0.8 kJ mol^{-1}. So the geometries optimized by the MPW1K function with the

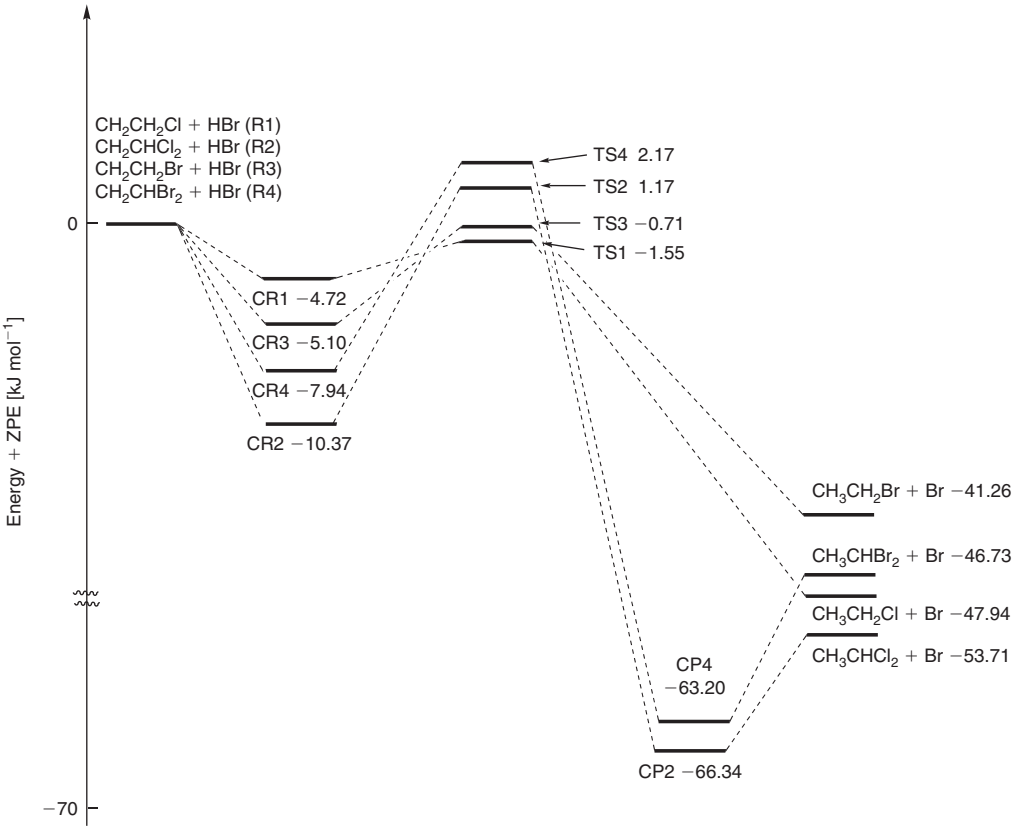

Fig. 2. Schematic pathways for the reactions R1–R4. Relative energies with zero-point energy (ZPE) at the G2M(RCC5)//MPW1K/6–311+G(d,p) level are in kJ mol^{-1}.

Table 2. Calculated barrier heights (in kJ mol^{-1}) for R1–R4 using various methods

Levels	R1	R2	R3	R4
G2M(RCC5)//MPW1K/6–311+G(d,p)	−1.55	1.17	−0.71	2.17
G2M(RCC5)//BMK/6–311+G(d,p)	−2.05	0.59	−0.92	1.88
G2M(RCC5)//MPW1K/6–311+G(2df,2p)	−1.42	1.21	−0.63	2.01
G2M(RCC5)//MPW1K/ma-TZVP	−1.30	1.38	−0.50	2.01

6–311+G(d,p) basis set are reliable in the present study. Thus, we employed the G2M(RCC5)//MPW1K/6–311+G(d,p) method to refine the potential energy surface and to calculate the rate constants.

Dynamic Calculations

Dual-level (X//Y) direct dynamics calculations were carried out for these reactions using the variational transition-state theory with interpolated single-point energies (VTST-ISPE)[26] approach. The rate constants for each reaction pathway were evaluated using the conventional transition-state theory (TST) and canonical variational transition-state theory (CVT)[27–29] over a wide temperature range of 200–2000 K. Tunnelling was corrected by means of the small-curvature tunnelling correction (SCT).[30,31]

The TST, CVT, CVT/SCT and available experimental rate constants for the reactions in the temperature range of 200–2000 K are presented in Fig. 3a–d. As the barrier heights of reactions R1 and R3 are negative, the tunnelling correction is not included for these two reactions. As shown in Fig. 3a, the TST rate constants are higher than the CVT ones in the temperature range 200–500 K, which means that the variational effect, which is defined as the ratio between the CVT and TST rate constants (k_{CVT}/k_{TST}), is important in the lower temperature range. With increasing temperature, the TST values become almost the same as the CVT ones, implying that the variational effect can become insignificant at higher temperatures. A similar conclusion can be reached for other reactions. What is the reason for this phenomenon? The classical potential energy curve ($V_{MEP}(s)$), the vibrationally adiabatic ground-state potential energy curve ($V_a^G(s)$) and the zero-point energy (ZPE) curve for reaction R1 as a function of the intrinsic reaction coordinate (s) are shown in Fig. 4. The maximum value of the potential energy profile at the G2M(RCC5)//MPW1K level is slightly shifted in the s direction; the saddle point position of the dual level is generally shifted under the VTST-ISPE scheme.[26] For reaction R1, the position of the maximum value of the $V_{MEP}(s)$ curve shifts towards the products ~0.54 Bohr, whereas the location of the maximum value of the $V_a^G(s)$ is still in the saddle point, i.e. $s = 0$. So the variational effect is larger when evaluating the rate constants for reaction R1. The other reactions produced a similar conclusion. With respect to reactions R2 and R4, the SCT corrections were considered. When comparing the CVT and CVT/SCT, the CVT/SCT rate constants are larger than CVT ones, especially at in the low-temperature range. The ratios of $k_{CVT/SCT}/k_{CVT}$ were 1.2 and 1.5 at 200 K for reactions R2 and R4 respectively.

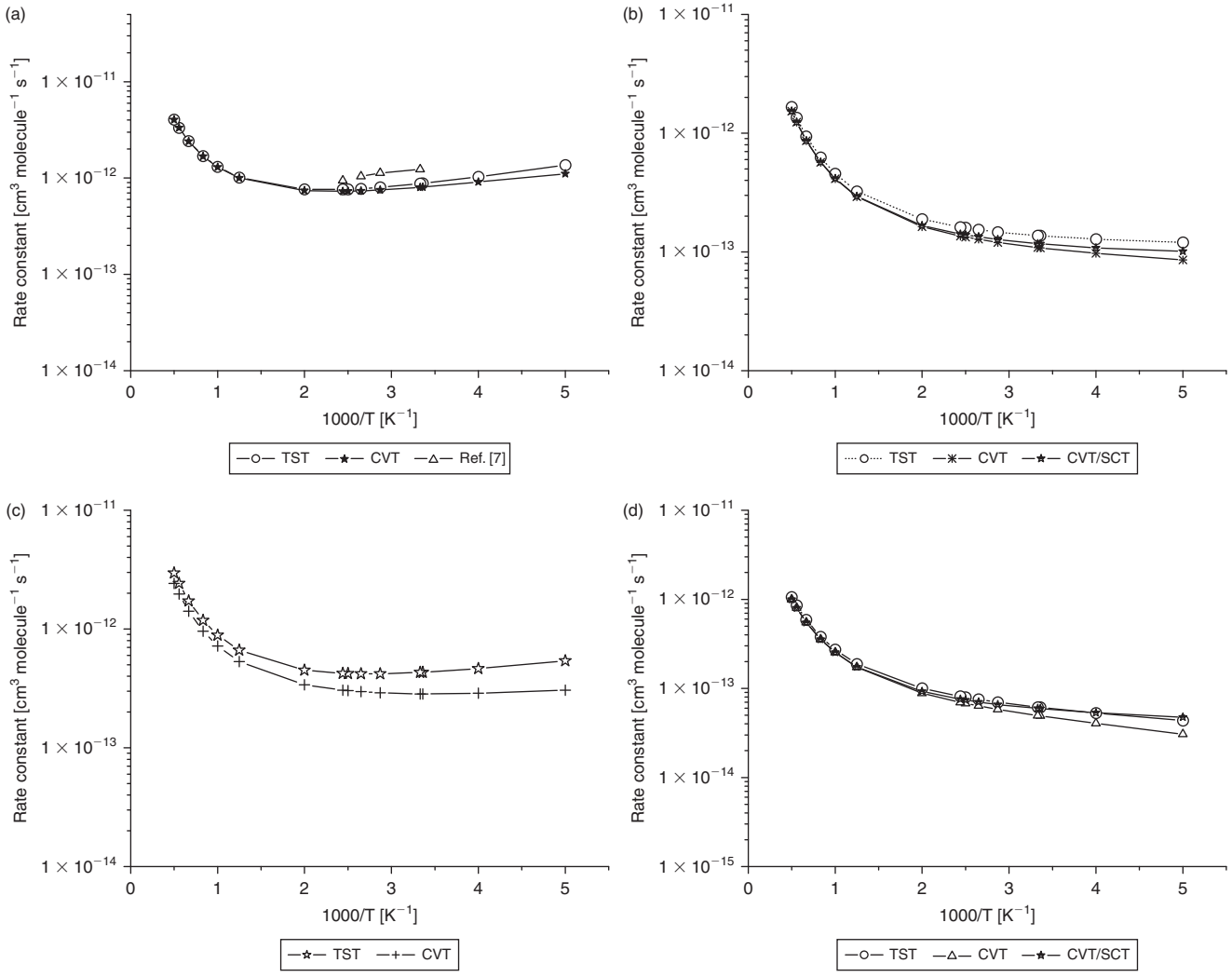

Fig. 3. (a) Plot of the TST and CVT theory rate constants calculated at the G2M(RCC5)//MPW1K/6–311+G(d,p) level along with the available experimental result[7] versus 1000/T between 200 and 2000 K for the reaction $CH_2CH_2Cl + HBr \rightarrow CH_3CH_2Cl + Br$ (R1). (b) Plot of the TST, CVT, and CVT/SCT (small-curvature tunnelling correction) rate constants calculated at the G2M(RCC5)//MPW1K/6–311+G(d,p) level versus 1000/T between 200 and 2000 K for the reaction $CH_2CHCl_2 + HBr \rightarrow CH_3CHCl_2 + Br$ (R2). (c) Plot of the TST and CVT rate constants calculated at the G2M(RCC5)//MPW1K/6–311+G(d,p) level versus 1000/T between 200 and 2000 K for the reaction $CH_2CH_2Br + HBr \rightarrow CH_3CH_2Br + Br$ (R3). (d) Plot of the TST, CVT, and CVT/SCT rate constants calculated at the G2M(RCC5)//MPW1K/6–311+G(d,p) level versus 1000/T between 200 and 2000 K for the reaction $CH_2CHBr_2 + HBr \rightarrow CH_3CHBr_2 + Br$ (R4). CVT: canonical variational transition-state; TST: transition-state theory; T: temperature.

For reaction R1, our calculated CVT rate constants are in good agreement with the experimental ones, with deviation within a factor of 1.3–1.5. Moreover, the calculated activation energy of $-0.92\,kJ\,mol^{-1}$ (300–409 K) agrees well with the corresponding experimental one of $-2.22 \pm 0.79\,kJ\,mol^{-1}$.[7] We obtained a negative temperature dependence, which is consistent with the experimental result. For reaction R3 with a negative barrier height, the rate constants also exhibit negative temperature dependence at the lower temperatures. As the calculated rate constants of reaction R1 agreed well with the available experimental values, it can be expected that the rate constants of reactions R2–R4 calculated at the same level are reliable, and these are shown in Fig. 3b–d.

Reactivity Trends

To evaluate the effect of chlorine or bromine substitution on reactivity, the rate constants of R1–R4 were plotted in Fig. 5. The experimental rate constants[32–36] of the reaction $C_2H_5 +$ HBr were also plotted in Fig. 5. The pre-exponential factors (A) and activation energies (E_a) were fitted based on the calculated CVT or CVT/SCT rate constants in the temperature range 200–500 K, and these are summarised in Table 3. Reactivity increases from chlorinated to non-chlorinated radicals for the ethyl radical: $\beta,\beta\text{-}C_2H_3Cl_2 < \beta\text{-}C_2H_4Cl < C_2H_5$. Note that the rate constants for $C_2H_5 +$ HBr were not calculated in this paper. The experimental rate constants were used for comparison. All experimental results were in good accordance with the above order except the result reported by Dobis et al.,[33] which is obviously lower than other experimental rate constants. The calculated activation energy of R1 ($-1.21\,kJ\,mol^{-1}$) is lower than that of R2 ($1.3\,kJ\,mol^{-1}$) by $2.5\,kJ\,mol^{-1}$, and the pre-exponential factor (A) of R1 is approximately two times higher than that of R2 (5.10×10^{-13} versus $2.07 \times 10^{-13}\,cm^3\,s^{-1}$). Thus, the increase in k stems from both the corresponding decrease in activation energy and increase in pre-exponential

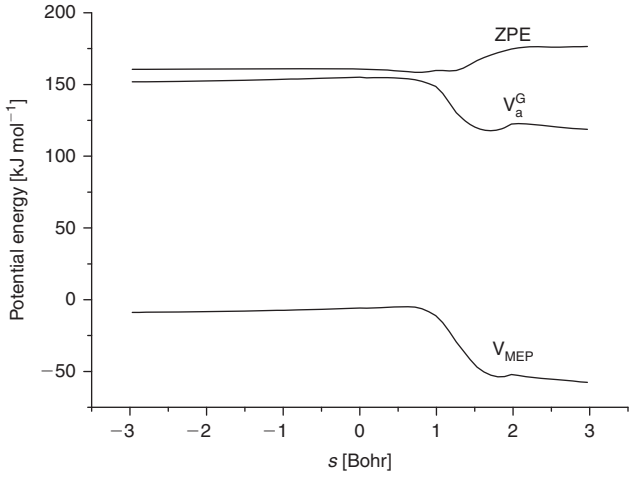

Fig. 4. Classical potential energy curve (V_{MEP}), ground-state vibrationally adiabatic energy curve (V_a^G), and zero-point energy (ZPE) curve as functions of s (Bohr) at the G2M(RCC5)//MPW1K/6–311+G(d,p) level for the reaction $CH_2CH_2Cl + HBr \rightarrow CH_3CH_2Cl + Br$ (R1).

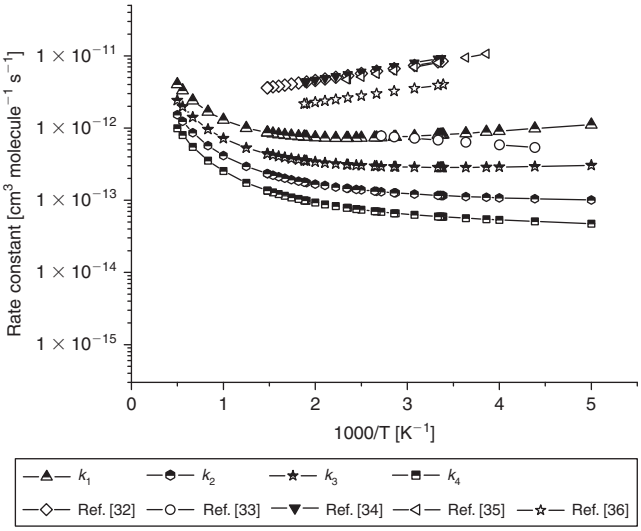

Fig. 5. Plot of the rate constants calculated at the G2M(RCC5)//MPW1K/6–311+G(d,p) level versus 1000/T between 200 and 2000 K for the reactions R1–R4 along with the experimental rate constants for the reaction $CH_3CH_2 + HBr \rightarrow CH_3CH_3 + Br$.[32–36]

Table 3. Arrhenius parameters for the title reactions in the temperature range 200–500 K

	A [cm^3 s^{-1}]	E_a [kJ mol^{-1}]
$CH_2CH_2Cl + HBr$ (R1)	5.10×10^{-13}	−1.21
$CH_2CHCl_2 + HBr$ (R2)	2.07×10^{-13}	1.30
$CH_2CH_2Br + HBr$ (R3)	3.23×10^{-13}	0.21
$CH_2CHBr_2 + HBr$ (R4)	1.26×10^{-13}	1.76

factor. A similar trend can be found for the brominated radicals. This suggests that the replacement of hydrogen by chlorine decreases the reactivity of the ethyl radical. However, when comparison is made between R1 and R3, the differences in both pre-exponetial factor (A) and activation energy (E_a) are smaller. The rate constants of R2 and R4 display similar trends.

Owing to the good agreement between the theoretical and experimental values, it is reasonable to believe that the present calculations provide reliable predictions of the rate constants for the title reactions over a large temperature range, which will be useful for modelling the combustion process and helping to assess their atmospheric lifetimes. Thus, the total rate constants of R1–R4 were fitted to the two modified Arrhenius equations to assist further experimental study. Table 4 lists the fitted parameters of the two modified Arrhenius equations for the same temperature range. Model 2, with one more parameter than Model 1, was recently reported by Zheng and Truhlar[37] to give a small error and correct low-temperature behaviour for the activation energy and rate constants.

Conclusion

In this paper, the hydrogen abstraction reactions of $CH_2CH_{3-n}X_n + HBr$ (X = Cl, Br and $n = 1, 2$) were studied by dual-level direct dynamics methods. Dynamics calculations were carried out using the VTST-ISPE method at the G2M(RCC5)//MPW1K/6–311+G(d,p) level. For all reactions, the variational effect is slightly larger in the low-temperature range, whereas the SCT effect plays an important role at a lower temperature for R2 and R4. We have provided reasonable theoretical values for the rate constants, which will be especially useful in the case of the reactions R2–R4, for which there are no well-determined experimental rate constants. Our calculation shows that chlorine or bromine substitution decreases the reactivity of ethyl radicals. The four-parameter expression is recommended because it gives smaller fitting errors and better low-temperature asymptotic behaviour.

Calculation Methods

All electronic structure calculations were carried out with the *Gaussian 09* program.[38] The equilibrium geometries of all the stationary points, including the reactants, transition states, complexes and products involved in the reactions, were calculated with the modified Perdew–Wang one-parameter model for kinetics (MPW1K)[39] with the 6–311+G(d,p) basis set (MPW1K/6–311+G(d,p)). To check the reliability of the results obtained at the MPW1K/6–311+G(d,p) level, the stationary geometries of reactions were optimized using the MPW1K functional with the 6–311+G(2df,2p) and ma-TZVP[25] basis sets and the BMK (Boese–Martin for Kinetics)[40] functional with the 6–311+G(d,p) basis set. The harmonic vibrational frequencies were calculated to characterise the nature of each critical point and to make ZPE corrections. Transition states showed only one negative eigenvalue in their diagonalized force constant matrices, and their associated eigenvectors were confirmed to correspond to the motion along the reaction coordinate under consideration, using the intrinsic reaction coordinate (IRC)[41] method in mass-weighted Cartesian coordinates. Also, first- and second-energy derivatives at geometries along the minimum-energy path (MEP) were obtained to calculate the curvature of the reaction path and the generalized vibrational frequencies along the reaction path. In order to obtain more accurate energies and barrier heights, single-point calculations were carried out by the modified *Gaussian-2* (G2M) method[42] with the optimized geometries. The dual-level potential profile along the reaction path was further refined with the interpolated single-point energies (ISPE) method.[26] Chuang and Truhlar[26] pointed out that at least four points are necessary to correct the low-energy-level reaction path: two points very close to the

Table 4. The fitted parameters using two modified Arrhenius equations for reactions R1–R4 in the temperature range 200–2000 K

	R1	R2	R3	R4
Model 1: $k = AT^n\exp(-E/RT)$				
A [s^{-1}]	7.66×10^{-19}	1.77×10^{-19}	4.01×10^{-19}	5.87×10^{-20}
n	1.98	2.06	2.01	2.15
E [kJ mol^{-1}]	−6.31	−3.97	−4.97	−3.76
Root mean square residual	0.06	0.04	0.04	0.05
Model 2: $k = AT^n\exp[-E(T+T_0)/R(T^2+T_0^2)]$				
A [s^{-1}]	5.33×10^{-20}	1.58×10^{-20}	5.59×10^{-20}	7.49×10^{-21}
n	2.33	2.38	2.27	2.42
E [kJ mol^{-1}]	−6.81	−4.77	−5.23	−4.35
T_0 [K]	158	175	155	171
Root mean square residual	0.01	0.01	0.01	0.02

saddle point that are used to locate the dual-level saddle point and two points close to the turning points for the tunnelling calculation. Except for these four non-stationary points (±0.05, ±1.0), for the present system, we also added the single-point energies of the reactant well or product well to correct the lower-level reaction path. Thus, the interpolation is based on single-point energies evaluated at seven points, namely reactant well, saddle point, product well (if existing), and four non-stationary points in the ISPE calculation.

The information on the potential energy surface was used to evaluate the rate constants by means of the *POLYRATE 9.7* program. The rate constants were calculated using the VTST[15–17] proposed by Truhlar and coworkers. The specific level of VTST that we used is CVT theory[27–29] or CVT with the SCT[30,31] method. The generalized normal-mode analysis was carried out in curvilinear coordinates.[43,44] The curvature components were calculated by using a quadratic fit to obtain the derivative of the gradient with respect to the reaction coordinate.

Supplementary Material

Cartesian coordinates, electronic energies, and frequencies calculated at several levels are available on the Journal's website.

Acknowledgements

We thank Professor Donald G. Truhlar for providing the *POLYRATE 9.7* program and the State Key Laboratory of Physical Chemistry of Solid Surfaces for providing computational resources. This work was supported by the National Natural Science Foundation of China (project no. 21003036), the Foundation for University Key Teachers from the He'nan Educational Committee, Science Foundation of He'nan Educational Committee (project nos. 2008A150005, 2011B150003), Science Foundation of He'nan University (project nos. 2009YBZR013, SBGJ090507) and Doctor Foundation of He'nan University.

References

[1] P. Beichert, L. Wingen, J. Lee, R. Vogt, M. J. Ezell, M. Ragains, R. Neavyn, B. J. Finlayson-Pitts, *J. Phys. Chem.* **1995**, *99*, 13156. doi:10.1021/J100035A018

[2] J. M. Nicovich, S. Wang, M. L. McKee, P. H. Wine, *J. Phys. Chem.* **1996**, *100*, 680. doi:10.1021/JP952396K

[3] L. Andrews, J. M. Dyke, N. Jonathan, N. Keddar, A. Morris, *J. Am. Chem. Soc.* **1984**, *106*, 299. doi:10.1021/JA00314A007

[4] J. A. Seetula, *J. Chem. Soc., Faraday Trans.* **1996**, *92*, 3069. doi:10.1039/FT9969203069

[5] K. Miyokawa, E. Tschuikow-Roux, *J. Phys. Chem.* **1990**, *94*, 715. doi:10.1021/J100365A037

[6] H. Q. He, J. Y. Liu, Z. S. Li, L. Wang, C. C. Sun, *J. Mol. Struc.-Theochem* **2008**, *859*, 30. doi:10.1016/J.THEOCHEM.2008.02.025

[7] J. A. Seetula, *J. Chem. Soc., Faraday Trans.* **1998**, *94*, 891. doi:10.1039/A706440C

[8] K. T. Wong, D. A. Armstrong, *Can. J. Chem.* **1969**, *47*, 4183. doi:10.1139/V69-692

[9] D. G. Truhlar, in *The Reaction Path in Chemistry: Current Approaches and Perspectives* **1995**, p. 229 (Ed. D. Heidrich) (Kluwer: Dordrecht, the Netherlands).

[10] D. G. Truhlar, B. C. Garrent, S. J. Klippenstein, *J. Phys. Chem.* **1996**, *100*, 12771. doi:10.1021/JP953748Q

[11] W. P. Hu, D. G. Truhlar, *J. Am. Chem. Soc.* **1996**, *118*, 860. doi:10.1021/JA952464G

[12] W. P. Hu, Y. P. Liu, D. G. Truhlar, *J. Chem. Soc., Faraday Trans.* **1994**, *90*, 1715. doi:10.1039/FT9949001715

[13] J. C. Corchado, E. L. Coitiño, Y. Y. Chang, P. L. Fast, D. G. Truhlar, *J. Phys. Chem. A* **1998**, *102*, 2424. doi:10.1021/JP9801267

[14] J. C. Corchado, Y. Y. Chuang, P. L. Past, W. P. Hu, Y. P. Liu, G. C. Lynch, K. A. Nguyen, C. F. Jackels, A. Fernandez-Ramos, B. A. Ellingson, B. J. Lynch, J. J. Zheng, V. S. Melissas, J. Villa, I. Rossi, E. L. Coitiño, J. Z. Pu, T. V. Albu, R. Steckler, B. C. Garrett, A. D. Isaacson, D. G. Truhlar, *POLYRATE, Version 9.7* **2007** (University of Minnesota: Minneapolis, MN).

[15] D. G. Truhlar, B. C. Garrett, *Acc. Chem. Res.* **1980**, *13*, 440. doi:10.1021/AR50156A002

[16] D. G. Truhlar, A. D. Isaacson, B. C. Garrett, in *The Theory of Chemical Reaction Dynamics* **1985**, p. 65 (Ed. M. Baer) (CRC Press: Boca Raton, FL).

[17] D. G. Truhlar, B. C. Garrett, *Annu. Rev. Phys. Chem.* **1984**, *35*, 159. doi:10.1146/ANNUREV.PC.35.100184.001111

[18] H. S. Tam, J. H. Choe, M. D. Harmony, *J. Phys. Chem.* **1991**, *95*, 9267. doi:10.1021/J100176A044

[19] C. Flanagan, L. Pierce, *J. Chem. Phys.* **1963**, *38*, 2963. doi:10.1063/1.1733627

[20] *NIST Chemistry Webbook* (Eds P. J. Linstrom, W. G. Mallard) Available online at: http://webbook.nist.gov/chemistry.

[21] T. Shimanouchi, *Tables of Molecular Vibrational Frequencies Consolidated Volume I* **1972** (National Bureau of Standards: Washington, DC).

[22] I. M. Alecu, J. J. Zheng, Y. Zhao, D. G. Truhlar, *J. Chem. Theory Comput.* **2010**, *6*, 2872. doi:10.1021/CT100326H

[23] W. B. DeMore, S. P. Sander, S. P. Golden, C. J. Howard, D. M. Golden, C. E. Kolb, R. F. Hampson, M. J. Molina, *Chemical Kinetics and Photochemical Data for Use in Stratospheric Modeling.* JPL Publication 97-4 **1997** (Jet Populsion Laboratory, NASA: Pasadena, CA).

[24] Y. R. Luo, *Comprehensive Handbook of Chemical Bond Energies* **2007** (CRC Press: Boca Raton, FL).

[25] J. J. Zheng, X. F. Xu, D. G. Truhlar, *Theor. Chem. Acc.* **2011**, *128*, 295. doi:10.1007/S00214-010-0846-Z
[26] Y. Y. Chuang, J. C. Corchado, D. G. Truhlar, *J. Phys. Chem.* **1999**, *103*, 2439. doi:10.1021/JP983750S
[27] B. C. Garrett, D. G. Truhlar, *J. Chem. Phys.* **1979**, *70*, 1593. doi:10.1063/1.437698
[28] B. C. Garrett, D. G. Truhlar, *J. Am. Chem. Soc.* **1979**, *101*, 4534. doi:10.1021/JA00510A019
[29] B. C. Garrett, D. G. Truhlar, R. S. Grev, A. W. Magnuson, *J. Phys. Chem.* **1980**, *84*, 1730. doi:10.1021/J100450A013
[30] D. H. Lu, T. N. Truong, V. S. Melissas, G. C. Lynch, Y. P. Liu, B. C. Garrett, R. Steckler, A. D. Issacson, S. N. Rai, G. C. Hancock, J. G. Lauderdale, T. Joseph, D. G. Truhlar, *Comput. Phys. Commun.* **1992**, *71*, 235. doi:10.1016/0010-4655(92)90012-N
[31] Y. P. Liu, G. C. Lynch, T. N. Truong, D. H. Lu, D. G. Truhlar, B. C. Garrett, *J. Am. Chem. Soc.* **1993**, *115*, 2408. doi:10.1021/JA00059A041
[32] J. A. Seetula, *J. Chem. Soc., Faraday Trans.* **1998**, *94*, 891. doi:10.1039/A706440C
[33] O. Dobis, S. W. Benson, *J. Phys. Chem. A* **1997**, *101*, 6030. doi:10.1021/JP970822R
[34] P. W. Seakins, M. J. Pilling, J. T. Niiranen, D. Gutman, L. N. Krasnoperov, *J. Phys. Chem.* **1992**, *96*, 9847. doi:10.1021/J100203A050
[35] J. M. Nicovich, C. A. Van Dijk, K. D. Kreutter, P. H. Wine, *J. Phys. Chem.* **1991**, *95*, 9890. doi:10.1021/J100177A051
[36] J. J. Russell, J. A. Seetula, D. Gutman, *J. Am. Chem. Soc.* **1988**, *110*, 3092. doi:10.1021/JA00218A017
[37] J. J. Zheng, D. G. Truhlar, *Phys. Chem. Chem. Phys.* **2010**, *12*, 7782. doi:10.1039/B927504E
[38] M. J. Frisch, G. W. Trucks, H. B. Schlegel, G. E. Scuseria, M. A. Robb, J. R. Cheeseman, G. Scalmani, V. Barone, B. Mennucci, G. A. Petersson, H. Nakatsuji, M. Caricato, X. Li, H. P. Hratchian, A. F. Izmaylov, J. Bloino, G. Zheng, J. L. Sonnenberg, M. Hada, M. Ehara, K. Toyota, R. Fukuda, J. Hasegawa, M. Ishida, T. Nakajima, Y. Honda, O. Kitao, H. Nakai, T. Vreven, Jr., J. A. Montgomery, J. E. Peralta, F. Ogliaro, M. Bearpark, J. J. Heyd, E. Brothers, K. N. Kudin, V. N. Staroverov, R. Kobayashi, J. Normand, K. Raghavachari, A. Rendell, J. C. Burant, S. S. Iyengar, J. Tomasi, M. Cossi, N. Rega, N. J. Millam, M. Klene, J. E. Knox, J. B. Cross, V. Bakken, C. Adamo, J. Jaramillo, R. Gomperts, R. E. Stratmann, O. Yazyev, A. J. Austin, R. Cammi, C. Pomelli, J. W. Ochterski, R. L. Martin, K. Morokuma, V. G. Zakrzewski, G. A. Voth, P. Salvador, J. J. Dannenberg, S. Dapprich, A. D. Daniels, Ö. Farkas, J. B. Foresman, J. V. Ortiz, J. Cioslowski, D. J. Fox, *Gaussian 09, Revision A.1* **2009** (Gaussian, Inc.: Wallingford, CT).
[39] B. J. Lynch, D. G. Truhlar, *J. Phys. Chem. A* **2001**, *105*, 2936. doi:10.1021/JP004262Z
[40] A. D. Boese, J. M. L. Martin, *J. Chem. Phys.* **2004**, *121*, 3405. doi:10.1063/1.1774975
[41] K. Fukui, *Acc. Chem. Res.* **1981**, *14*, 363. doi:10.1021/AR00072A001
[42] A. M. Mebel, K. Morokuma, M. C. Lin, *J. Chem. Phys.* **1995**, *103*, 7414. doi:10.1063/1.470313
[43] C. F. Jackels, Z. Gu, D. G. Truhlar, *J. Chem. Phys.* **1995**, *102*, 3188. doi:10.1063/1.468630
[44] Y.-Y. Chuang, D. G. Truhlar, *J. Phys. Chem.* **1997**, *101*, 3808. doi:10.1021/JP970052J